

1

## Supporting Information (SI)

2 **Efficient Removal of Both Antimonite (Sb(III)) and Antimonate**

3 **(Sb(V)) from Environmental Water Using Titanate nanotubes**

4 **and nanoparticles**

5

6 Tianhui Zhao,<sup>ab</sup> Zhi Tang,<sup>a</sup> Xiaoli Zhao,<sup>\*a</sup> Hua Zhang,<sup>a</sup> Junyu Wang,<sup>ab</sup> Fengchang Wu,<sup>a</sup>

7 John P. Giesy,<sup>c</sup> Jia Shi.<sup>d</sup>

8 <sup>a</sup> State Key Laboratory of Environmental Criteria and Risk Assessment, Chinese

9 Research Academy of Environmental Sciences, Beijing 100012, China.

10 <sup>b</sup> College of Water Sciences, Beijing Normal University, Beijing 100875, China.

11 <sup>c</sup> Department of Veterinary Biomedical Sciences and Toxicology Centre, University

12 of Saskatchewan, Saskatoon, Saskatchewan, Canada.

13 <sup>d</sup> University of Science and Technology, Beijing, 100083, China

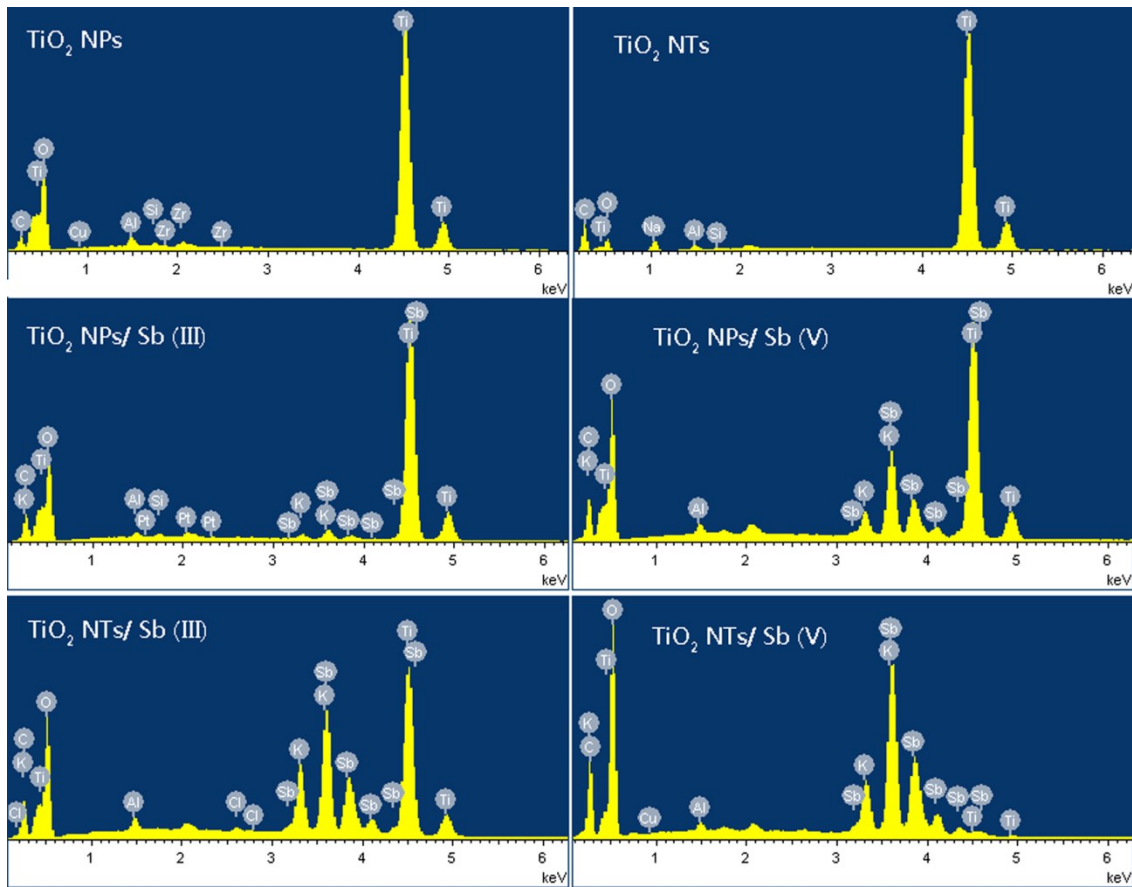
14 Corresponding author.

15 E-mail: [zhaoxiaoli\\_zxl@126.com](mailto:zhaoxiaoli_zxl@126.com)

16

17 Supplemental Information, 19 pages with 10 Figures and 4 Tables

18

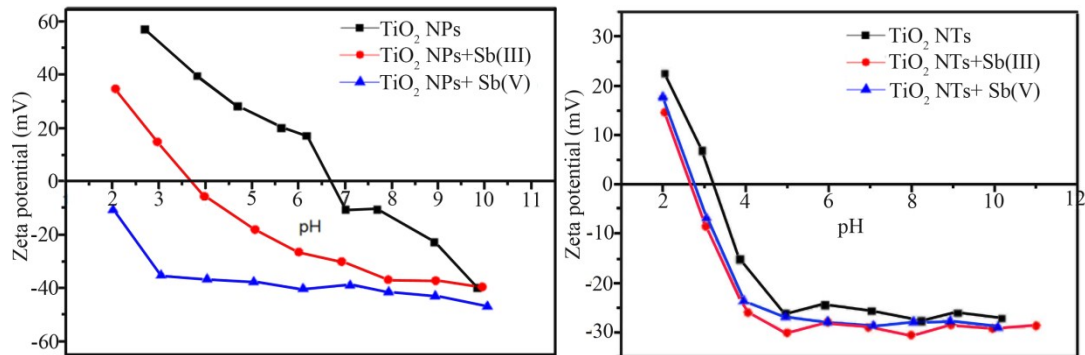


19

20 **Fig.S1 EDX spectras of  $\text{TiO}_2$  NPs,  $\text{TiO}_2$  NTs,  $\text{TiO}_2$  NPs/ Sb (III),  
21  $\text{TiO}_2$  NPs/ Sb (V),  $\text{TiO}_2$  NTs/ Sb (III),  $\text{TiO}_2$  NTs/ Sb (V)**

22

23 Fig.S2 Changes of Zeta potentials of  $\text{TiO}_2$  NPs and  $\text{TiO}_2$  NTs before and after  
 24 adsorbing Sb(III) and Sb(V). Adsorption capacity of  $\text{TiO}_2$  NTs is greater than that of  
 25  $\text{TiO}_2$  NPs. To compare adsorption of Sb(III) or Sb(V) on surfaces of  $\text{TiO}_2$  NPs or  $\text{TiO}_2$   
 26 NTs, changes of Zeta potential of  $\text{TiO}_2$  NTs was less than for  $\text{TiO}_2$  NPs. Electrostatic  
 27 interactions are the primary mechanism of adsorption of Sb(V) on  $\text{TiO}_2$  NMNs.  
 28 Positive charges on surfaces of  $\text{TiO}_2$  NMNs were neutralized by compounds of Sb(V).  
 29 Meanwhile, complexation played a dominant role in adsorption of Sb (III) on  $\text{TiO}_2$   
 30 NMNs. Changes of Zeta potential of Sb(V) adsorbed onto  $\text{TiO}_2$  NMNs may be due to  
 31 forming a stable inner complex.<sup>14,15</sup>



32  
 33 **Fig.S2 Zeta potentials of adsorption of Sb(III) and Sb(V) on  $\text{TiO}_2$  NPs and  $\text{TiO}_2$**   
 34 **NTs**  
 35

36 The Dubinin–Radushkevich (D-R) isotherm model can be used to determine the  
37 nature of the adsorption process (physical or chemical).<sup>11</sup> The linear equation of the  
38 D-R isotherm is expressed as Equation 1 and 2:<sup>15</sup>

39  $\ln Q_e = \ln Q_{DR} - \beta \varepsilon^2$  (1)

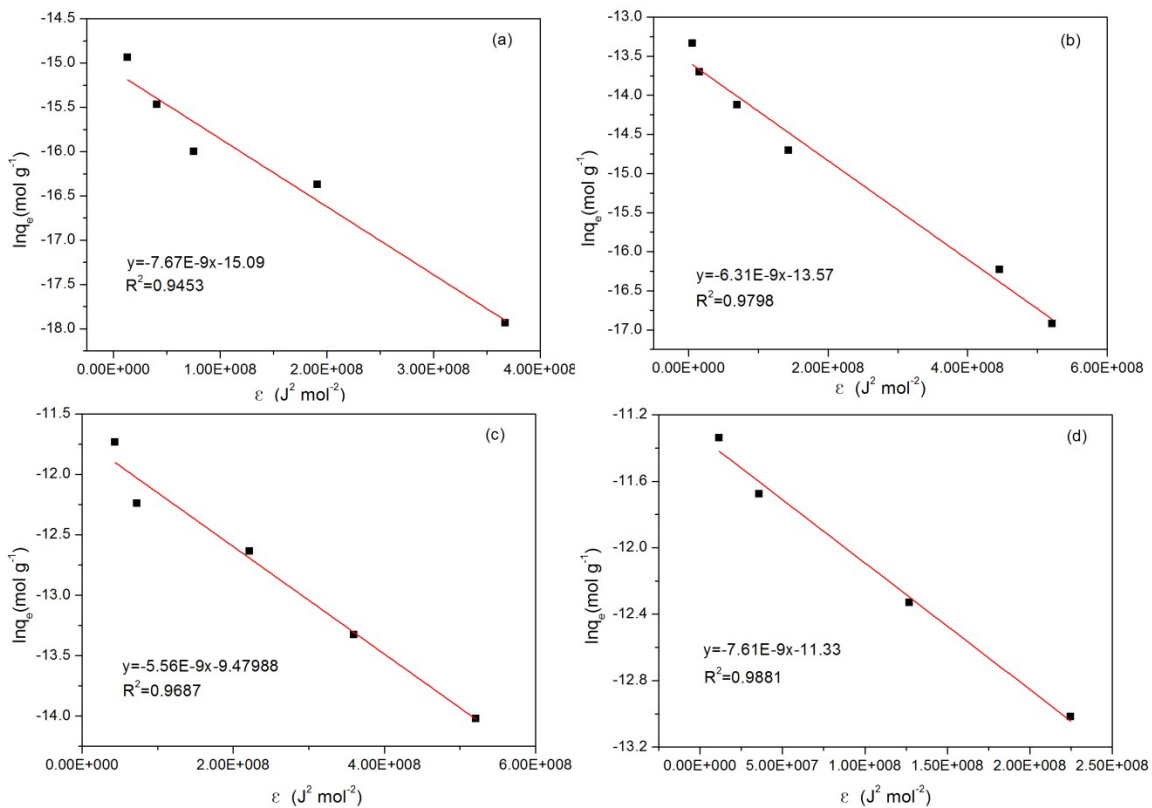
40  $\varepsilon = RT \ln (1 + 1/C_e)$  (2)

41 where  $q_e$  is the amount of metal ions sorbed per unit weight of adsorbent (mol  
42 L<sup>-1</sup>),  $q_m$  is the maximum adsorption capacity (mol g<sup>-1</sup>),  $\beta$  is the activity coefficient  
43 related to the mean free energy of adsorption (mol<sup>2</sup> J<sup>-2</sup>), R is the gas constant (8.314 J  
44 (mol K)<sup>-1</sup>); T is the thermodynamic temperature (K); and  $\varepsilon$  is the Polanyi potential.

45 The D-R isotherm model fits the equilibrium data well (Figure S3 and Table S2),  
46 R<sup>2</sup> values were 0.95, 0.98, 0.97, 0.99 for Sb(III) and Sb(V) adsorption on TiO<sub>2</sub> NPs  
47 and TiO<sub>2</sub> NTs, respectively. The mean free energy of adsorption (E; kJ (J mol)<sup>-1</sup>) is  
48 expressed as Equation 3:

49  $E = \frac{1}{\sqrt{2\beta}}$  (3)

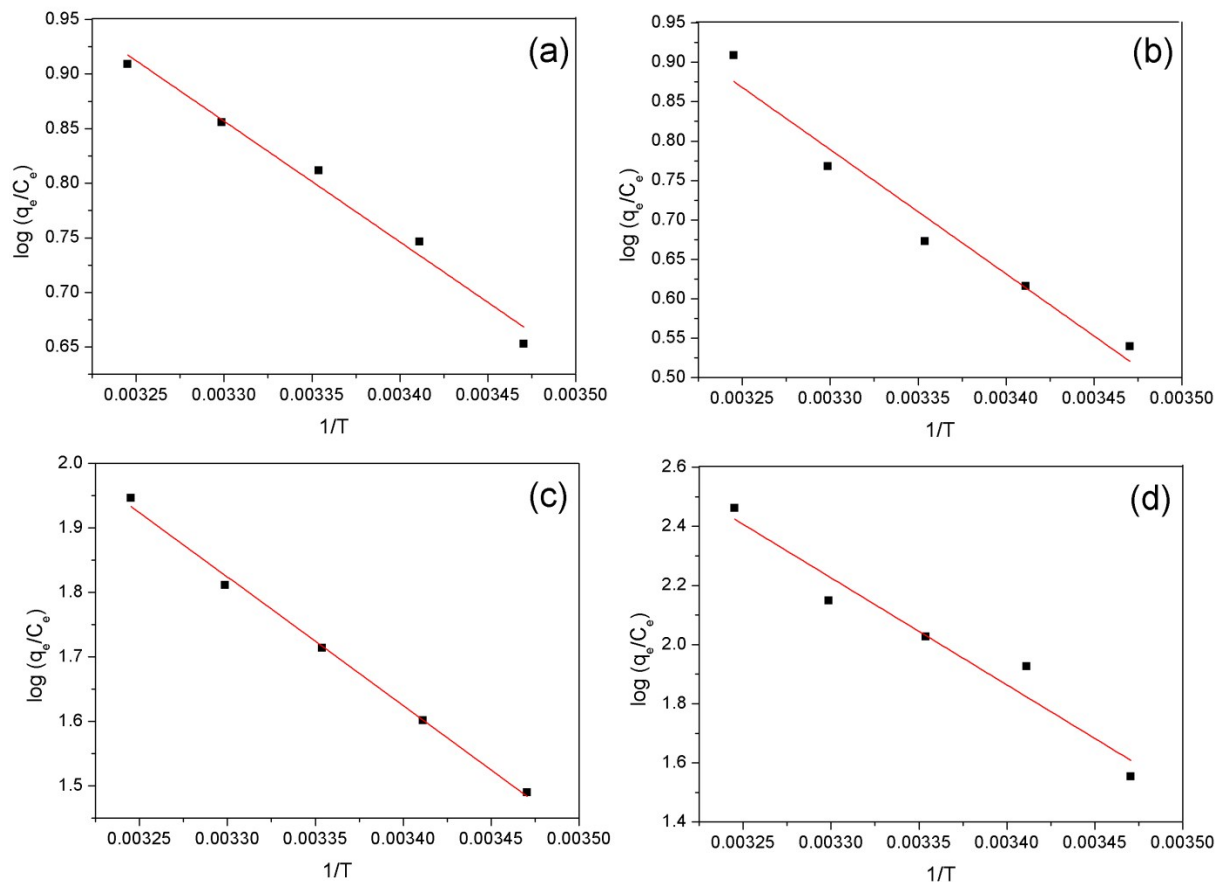
50 The adsorption behavior might be predicted, whether physical or chemical  
51 process, from the E value, which in the range of 8-16 kJ mol<sup>-1</sup> is ion-exchange  
52 reaction. The mean free energy of Sb(III) and Sb(V) adsorption on TiO<sub>2</sub> NPs were  
53 8.07, 8.90 kJ mol<sup>-1</sup> and on TiO<sub>2</sub> NTs were 9.48 and 8.11 kJ mol<sup>-1</sup>, respectively, which  
54 indicated the both Sb(III) and Sb(V) adsorption are chemical process in nature.



55

56 **Fig.S3 Dubinin–Radushkevich (D-R) isotherm models of Sb(III) adsorbed on**  
 57 **TiO<sub>2</sub> NPs (a), Sb(V) on TiO<sub>2</sub> NPs (b), Sb(III) on TiO<sub>2</sub> NTs (c), Sb(V) on TiO<sub>2</sub> NTs**  
 58 **(d). adsorbent dose was 5 mg; the solution volume was 50 mL; pH was 2.2 ± 0.1**

59

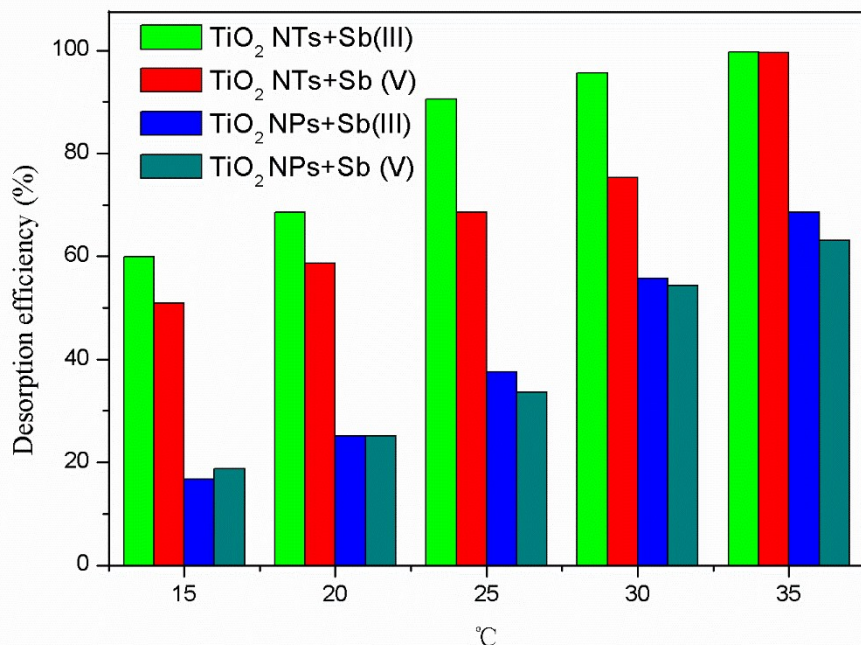


60

61 **Fig.S4 Adsorption thermodynamics of Sb(III) adsorbed on  $\text{TiO}_2$  NPs (a), Sb(V)  
62 on  $\text{TiO}_2$  NPs (b), Sb(III) on  $\text{TiO}_2$  NTs (c), Sb(V) on  $\text{TiO}_2$  NTs (d). adsorbent dose  
63 was 5 mg; the solution volume was 50 mL; pH was  $2.2 \pm 0.1$ ; The temperature**

64 was 15, 20, 25, 30, 35 °C

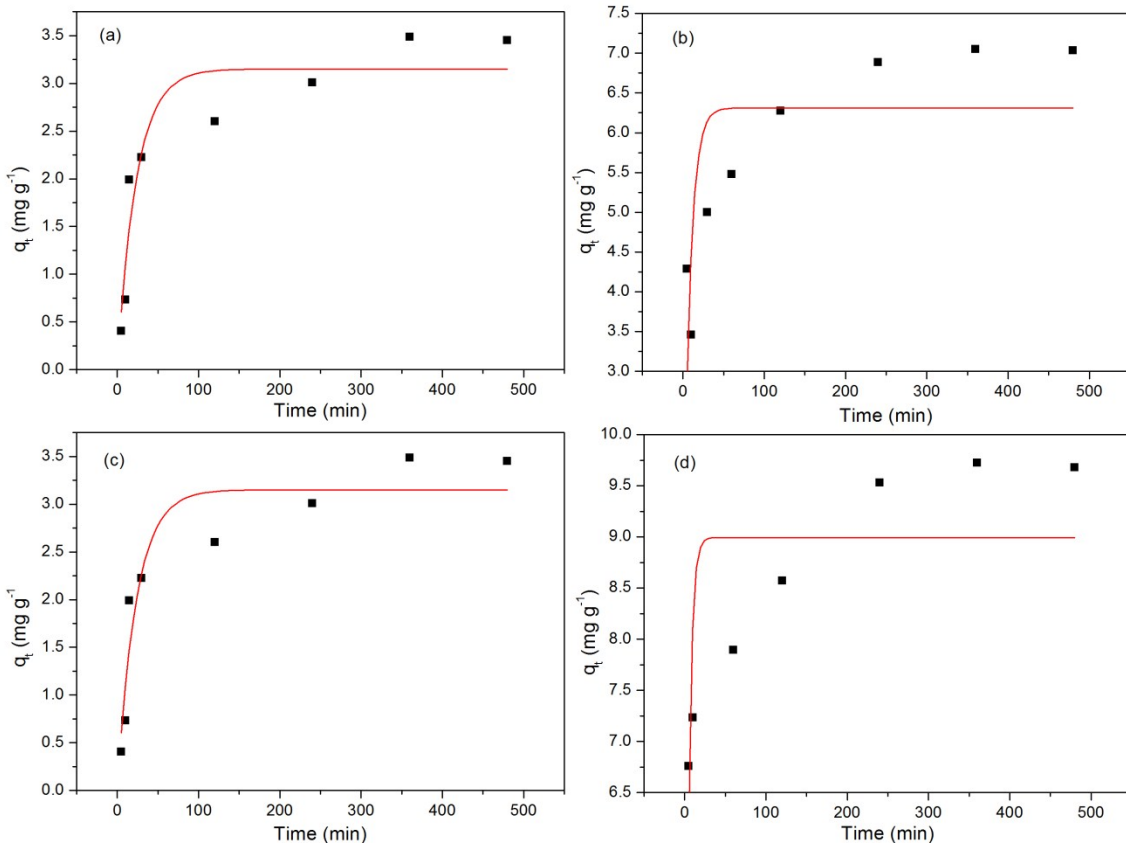
65



66

67 **Fig.S5 Desorption thermodynamics of Sb(III) adsorbed on TiO<sub>2</sub> NPs, Sb(V) on**  
 68 **TiO<sub>2</sub> NPs, Sb(III) on TiO<sub>2</sub> NTs, Sb(V) on TiO<sub>2</sub> NTs.** adsorbent dose was 5 mg;  
 69 the solution volume was 50 mL; desorbing agent was 0.1 mol L<sup>-1</sup> NaOH; The  
 70 temperature was 15, 20, 25, 30, 35 °C

71



72  
 73 **Fig.S6 Pseudo-first-order kinetic curves of Sb(III) adsorbed on TiO<sub>2</sub> NPs (a),**  
 74 **Sb(V) on TiO<sub>2</sub> NPs (b) , Sb(III) on TiO<sub>2</sub> NTs (c), Sb(V) on TiO<sub>2</sub> NTs (d).** Initial  
 75 **Sb(III) and Sb(V) concentration was 10 µg L<sup>-1</sup> - 10 mg L<sup>-1</sup>; adsorbent dose was 5**  
 76 **mg; the solution volume was 50 mL; and pH was 2.2 ± 0.1**

77

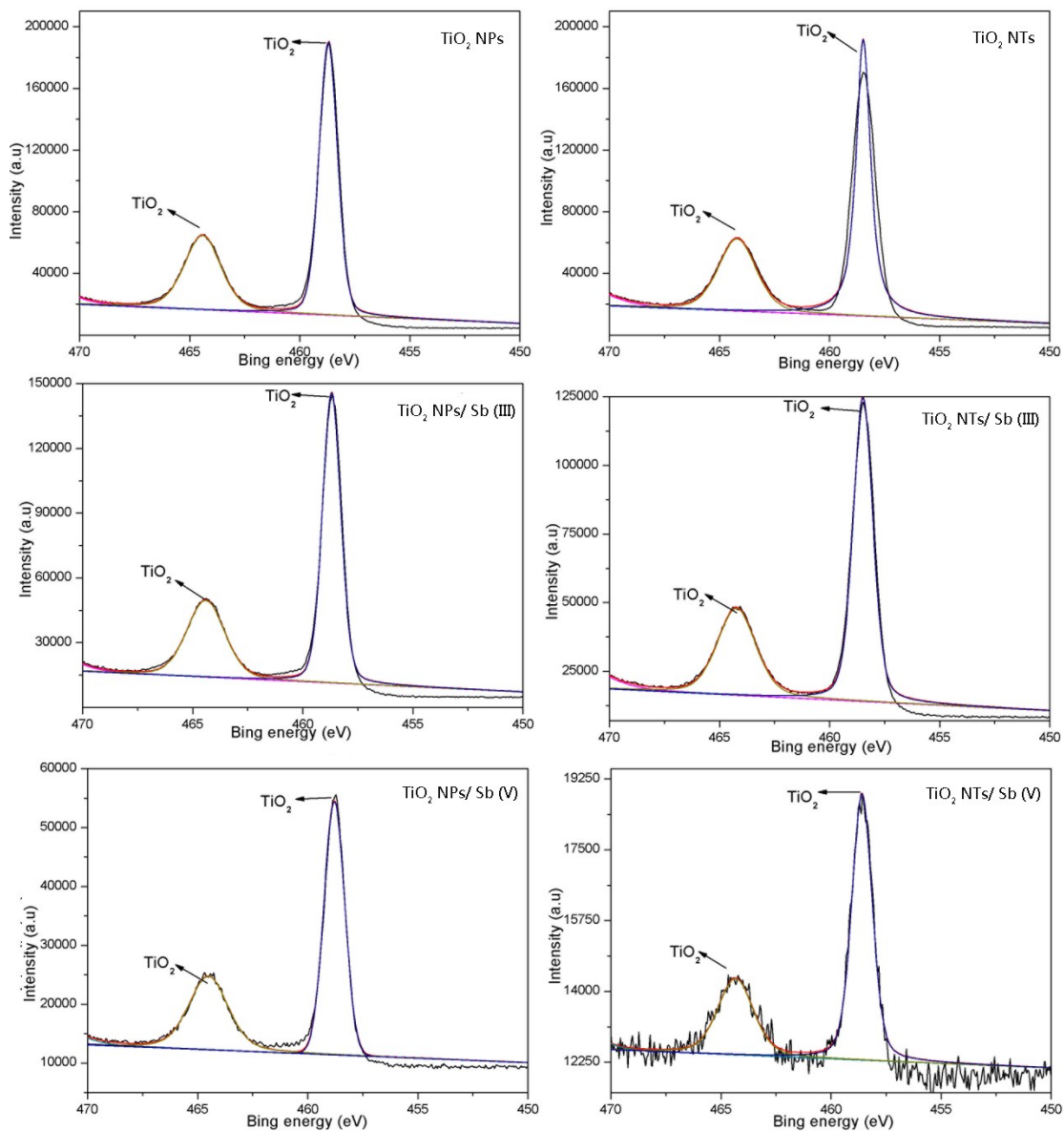
78       Pseudo-first-order kinetic models are expressed as Equation 4:

79

$$q_t = q_e (1 - e^{-k_1 t}) \quad (4)$$

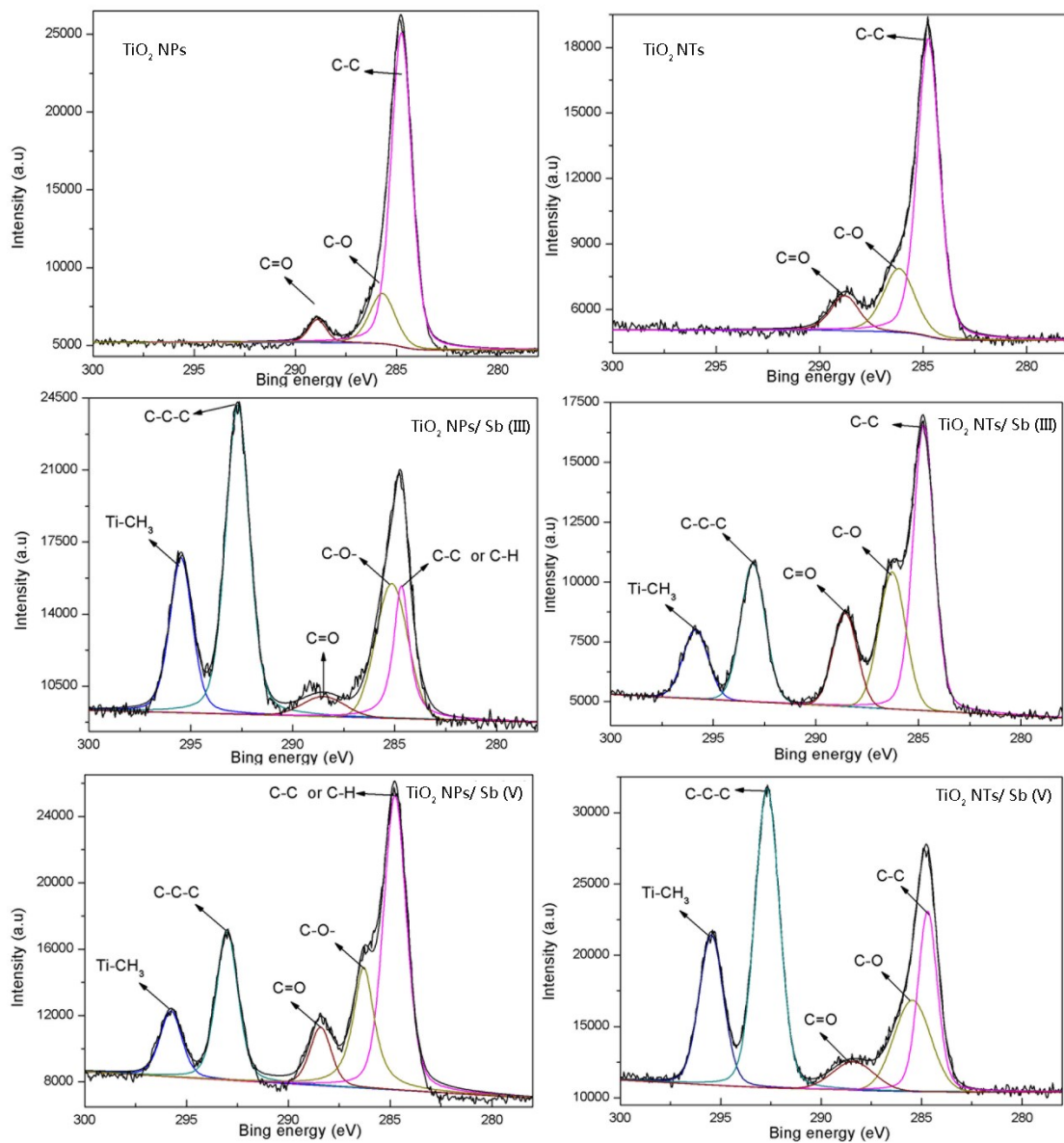
80       Where q<sub>e</sub> is the amount of adsorbate at equilibrium (mg g<sup>-1</sup>); q<sub>t</sub> is the amount of  
 81 adsorbate (mg g<sup>-1</sup>) at time t (min); and K<sub>1</sub> (min<sup>-1</sup>) and K<sub>2</sub> (g mg·min<sup>-1</sup>) are the rate  
 82 constants for the pseudo first-order sorption, respectively.

83



86 **Fig.S7 XPS spectras of Ti for  $\text{TiO}_2$  NPs,  $\text{TiO}_2$  NTs,  $\text{TiO}_2$  NPs/ Sb (III),  $\text{TiO}_2$  NPs/**

87 Sb (V),  $\text{TiO}_2$  NTs/ Sb (III),  $\text{TiO}_2$  NTs/ Sb (V)



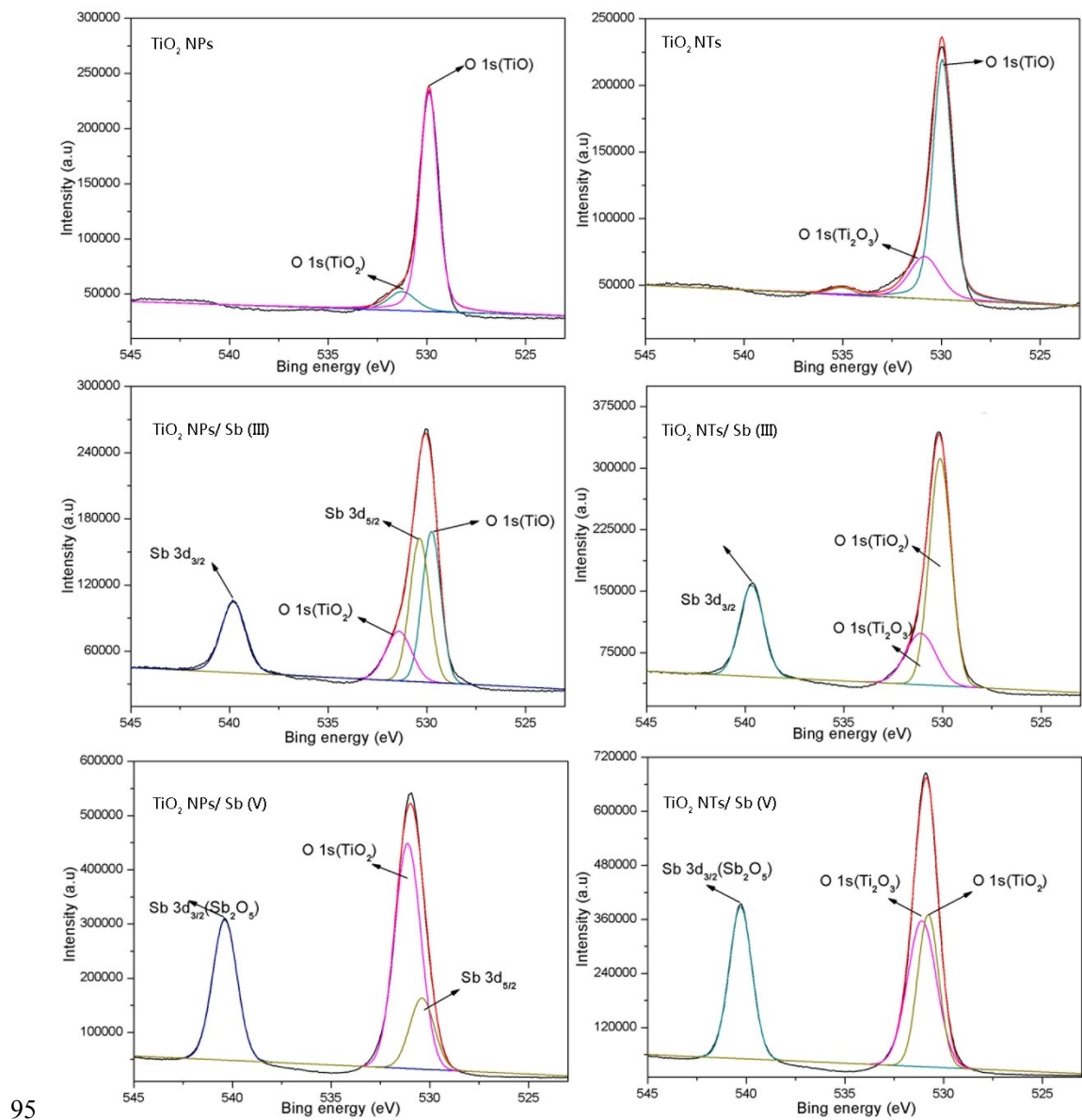
89

90 **Fig.S8 XPS spectras of C1s for  $\text{TiO}_2$  NPs,  $\text{TiO}_2$  NTs,  $\text{TiO}_2$  NPs/ Sb (III),  $\text{TiO}_2$   
91 NPs/ Sb (V),  $\text{TiO}_2$  NTs/ Sb (III),  $\text{TiO}_2$  NTs/ Sb (V)**

92

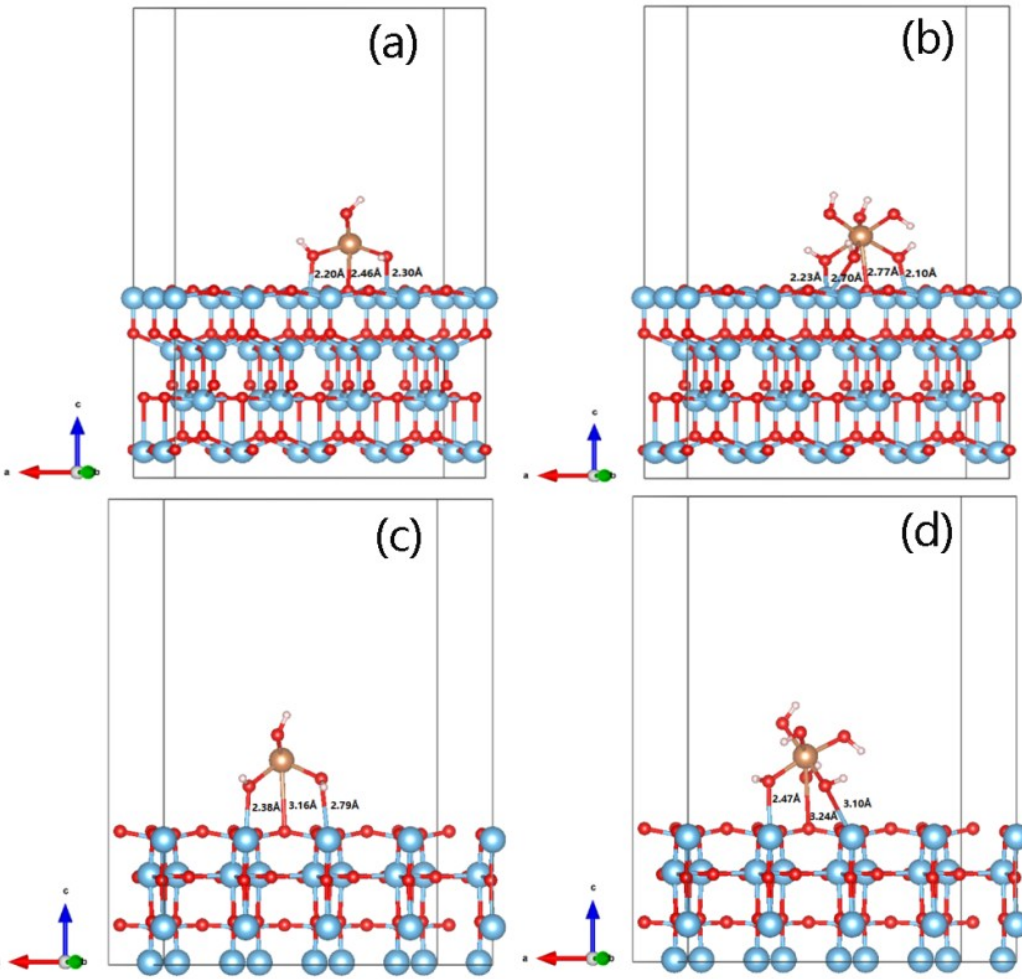
93

94



96 **Fig.S9 XPS spectras of O1s for TiO<sub>2</sub> NPs, TiO<sub>2</sub> NTs, TiO<sub>2</sub> NPs/ Sb (III), TiO<sub>2</sub>  
97 NPs/ Sb (V), TiO<sub>2</sub> NTs/ Sb (III), TiO<sub>2</sub> NTs/ Sb (V)**

98



99  
100 **Fig.S10 Optimized  $\text{TiO}_2$  {001} plane slab models for Sb(III) adsorption (a) and**  
101 **Sb(V) adsorption (b), optimized  $\text{TiO}_2$  {100} plane slab models for Sb(III)**  
102 **adsorption (c) and Sb(V) adsorption (d)**

103

104 As shown in Figure. 10a, two O atoms of Sb(III) bond with two Ti atoms. The  
105 bond length of Ti-O is 2.20 and 2.30 Å, respectively. As shown in Figure. 10b, three  
106 O atoms of Sb(V) bond with two Ti atoms, the Ti-O length is 2.10 Å, 2.23 Å and 2.70  
107 Å, respectively.

108 Comparing to adsorption results of {001} facet, Sb(III) and Sb(V) adsorbed on  
109 {100} facet is slightly loose. As shown in Figure 10c and 10d, the adsorption pattern  
110 of Sb(III) adsorbed on {100} facet is same with the {001} facet. The Ti-O bond  
111 length is 2.38 Å and 2.79 Å. The two O atoms of Sb(V) adsorbed on Ti atoms  
112 respectively, Ti-O bond length is 2.47 Å and 3.10 Å.

113

**Table S1 Comparison of performance of TiO<sub>2</sub> NTs (present study) and various adsorbents for removal of Sb from water.**

114

Adsorbents	Concentration range (initial concentration mg L <sup>-1</sup> )	pH	Dose (g L <sup>-1</sup> )	Adsorption amount (mg g <sup>-1</sup> )		References
				Sb (III)	Sb (V)	
TiO <sub>2</sub> NTs(Present study)	0.01-10	2.0-10.0	0.1	250.00	56.30	-
carbon nanofibers decorated with zirconium oxide (ZrO <sub>2</sub> )	10-500	7.0 ± 0.2	1.0	70.83	57.17	1
Activated alumina	5-75	2.0-11.0	1.0	-	38.00	2
Nanoscale zero-valent iron	0-20	4.0-10.0	2.0	6.99	1.65	3
Hematite coated magnetic nanoparticle	1-20	4.1	0.1	36.70	-	4
Synthetic manganite	0.5-98	3.0	0.6	-	95.00	5
Iron-zirconium bimetal oxide	0-25	7.0	0.2	-	51.00	6
α-FeOOH	-	2.0-12.0	25.0	-	48.70	7
Kaolinite	1	6.0	25.0	-	12.00	8
Diatomite	10-400	6.0	4.0	35.20	-	9

Cyanobacteria	10	2.0–7.0	0.8–20.0	4.88	-	10
Zr-MOFs	2–500	2.3–9.5	0.8	136.97	287.88	11
$\alpha$ -MnO <sub>2</sub> Nanofibers	10–500	4.0	0.5	111.70	89.99	12
Reduced graphene oxides/Mn <sub>3</sub> O <sub>4</sub>	10–1000	2.5–11.5	1.0	151.84	105.50	13

116

**Table S2 D-R isotherm parameters for Sb(III) and Sb(V) adsorption on TiO<sub>2</sub> NPs and TiO<sub>2</sub> NTs.**

Adsorbed types	D-R isotherm model		
	q <sub>m'</sub> (mol g <sup>-1</sup> )	β (mol <sup>2</sup> J <sup>-2</sup> )	R <sup>2</sup>
Sb(III)+ TiO <sub>2</sub> NPs	1.24 × 10 <sup>-7</sup>	7.67 × 10 <sup>-9</sup>	0.95
Sb(V)+ TiO <sub>2</sub> NPs	1.28 × 10 <sup>-6</sup>	6.31 × 10 <sup>-9</sup>	0.98
Sb(III)+ TiO <sub>2</sub> NTs	7.64 × 10 <sup>-5</sup>	5.56 × 10 <sup>-9</sup>	0.97
Sb(V)+ TiO <sub>2</sub> NTs	1.20 × 10 <sup>-5</sup>	7.61 × 10 <sup>-9</sup>	0.99

117

**Table S3 Thermodynamics of adsorption of Sb(III) and Sb(V) on TiO<sub>2</sub> NPs and TiO<sub>2</sub> NTs**

Adsorbed types	$-\Delta G^0(\text{KJ mol}^{-1})$						
	$\Delta H^0$ (KJ mol <sup>-1</sup> )	$\Delta S^0$ (J mol <sup>-1</sup> K <sup>-1</sup> )	15°C	20°C	25°C	30°C	35°C
Sb(III)+TiO <sub>2</sub> NPs	1.11	4.51	0.19	0.21	0.23	0.26	0.28
Sb(V)+TiO <sub>2</sub> NPs	1.58	5.98	0.14	0.17	0.20	0.23	0.26
Sb(V)+TiO <sub>2</sub> NTs	3.62	14.18	0.47	0.54	0.61	0.68	0.75
Sb(III)+TiO <sub>2</sub> NTs	1.99	8.40	0.43	0.47	0.51	0.56	0.60

120

**Table S4 Efficiencies of removal of Sb by TiO<sub>2</sub> NMIs in natural water**

Real water	TOC mg L <sup>-1</sup>	UV 465/665	TiO <sub>2</sub> NPs/Sb(III)		TiO <sub>2</sub> NPs/Sb(V)		TiO <sub>2</sub> NTs/Sb(III)		TiO <sub>2</sub> NTs/Sb(V)	
			Adsorbed amount (mg g <sup>-1</sup> )	Removal efficiency (%)						
Tap water	3.62	0.032	104.63	52	89.44	44	199.88	100	199.58	100
Landscape water	10.83	0.076	68.64	34	30.49	15	199.64	100	198.13	99
Treatment plant effluent	20.85	0.228	82.93	41	47.80	23	199.82	100	113.66	57

121

122 **References**

- 123 1 J.M. Luo, X.B. Luo, J. Crittenden, J.H. Qu, Y.H. Bai, Y. Peng and J.H. Li, Removal  
124 of antimonite (Sb(III)) and antimonate (Sb(V)) from aqueous solution using carbon  
125 nanofibers that are decorated with zirconium oxide ( $ZrO_2$ ), *Environ. Sci. Technol.*,  
126 2015, **49**, 11115-11124.
- 127 2 Y.H. Xu, A. Ohki and S. Maeda, Adsorption and removal of antimony from  
128 aqueous solution by an activated alumina, *Toxicol. Environ. Chem.*, 2001, **80**, 145-  
129 154.
- 130 3 X.Q. Zhao, X.M. Dou, D. Mohan, C.U. Pittman Jr, S.O. Yong and X. Jin,  
131 Antimonate and antimonite adsorption by a polyvinyl alcohol-stabilized granular  
132 adsorbent containing nanoscale zero-valent iron, *Chem. Eng. J.*, 2014, **247**, 250-257.
- 133 4 C. Shan, Z.Y Ma and M.P Tong, Efficient removal of trace antimony(III) through  
134 adsorption by hematite modified magnetic nanoparticles, *J. Hazard. Mater.*, 2014,  
135 **268**, 229-236.
- 136 5 X.Q. Wang, M.C. He, C.Y. Lin, Y.X. Gao and L. Zheng, Antimony(III) oxidation  
137 and antimony(V) adsorption reactions on synthetic manganite, *Chem. Erde.  
Geochem.*, 2012, **72**, 41-47.
- 139 6 X.H. Li, X.M. Dou and J.Q. Li, Antimony(V) removal from water by iron -  
140 zirconium bimetal oxide: performance and mechanism, *J. Environ. Sci.*, 2012, **24**,  
141 1197-1203.
- 142 7 X.J. Guo, Z.J. Wu, M.C. He, X.G. Meng, X. Jin, N. Qiu and J. Zhang, Adsorption  
143 of antimony onto iron oxyhydroxides: adsorption behavior and surface structure, *J.  
Hazard. Mater.*, 2014, **276**, 339-345.
- 145 8 J.H. Xi, M.C. He and C.Y. Lin, Adsorption of antimony(V) on kaolinite as a  
146 function of pH, ionic strength and humic acid, *Environ. Earth. Sci.*, 2010, **60**, 715-  
147 722.
- 148 9 A. Sari, D. Çitak, M. Tuzen, Equilibrium, thermodynamic and kinetic studies on  
149 adsorption of Sb(III) from aqueous solution using low-cost natural diatomite, *Chem.  
Eng. J.*, 2010, **162**, 521-527.
- 151 10 F.C. Wu, F.H. Sun, S. Wu, Y.B. Yan and B.S. Xing, Removal of antimony(III)  
152 from aqueous solution by freshwater cyanobacteria *Microcystis* biomass, *Chem.  
Eng. J.*, 2012, **183**, 172-179
- 154 11 J. Li, X.D. Li, T. Hayat, A. Alsaedi and C.L. Chen, Screening of zirconium-based  
155 metal-organic frameworks for efficiently simultaneous removal of antimonite  
156 (Sb(III)) and antimonate (Sb(V)) from aqueous solution, *Acs. Sustain. Chem. Eng.*,  
157 2017, **5**, 11496-11503.
- 158 12 J.M. Luo, C.Z. Hu, X.Y. Meng, J. Crittenden, J.H. Qu, and P. Peng, Antimony  
159 removal from aqueous solution using novel  $\alpha\text{-MnO}_2$  nanofibers: equilibrium,  
160 kinetic, and density functional theory studies, *Acs. Sustain. Chem. Eng.*, 2017, **5**,  
161 2255-2264.
- 162 13 J.P. Zou, H.L. Liu, J.M. Luo, Q.J. Xing, H.M. Du, X.H. Jiang, X.B. Luo, S.L. Luo,  
163 and S.L. L. Suib, Three-Dimensional reduced graphene oxide coupled with  $Mn_3O_4$   
164 for highly efficient removal of Sb(III) and Sb(V) from water, *Acs. Appl. Mater.  
Interfaces*, 2016, **8**, 18140-18149.

- 166 14 M. Pena, X. Meng, G.P. Korfiatis and C. Jing, Adsorption mechanism of arsenic  
167 on nanocrystalline titanium dioxide, *Environ. Sci. Technol.*, 2006, **40**, 1257-1262.  
168 15 A.H. Chen, S.C. Liu, C.Y. Chen, C.Y. Chen, Comparative adsorption of Cu(II),  
169 Zn(II), and Pb(II) ions in aqueous solution on the crosslinked chitosan with  
170 epichlorohydrin. *J. Hazard. Mater.*, 2008, **154**, 184-91.  
171